

Photoinduced multiple microchannels inside silicon produced by a femtosecond laser

C. Li · X. Shi · J. Si · F. Chen · T. Chen · Y. Zhang ·
X. Hou

Received: 22 June 2009 / Revised version: 24 August 2009 / Published online: 19 September 2009
© Springer-Verlag 2009

Abstract Photoinduced multiple microchannels in the interior of silicon produced by an 800-nm femtosecond laser were observed. The multiple microchannels were aligned spontaneously with a period along the propagation direction of the laser beam, which could be attributed to the interface spherical aberration induced due to refractive-index mismatch. We also observed that the depth of the photoinduced microchannels increased with the increase of the laser power. The power dependence of the depth of photoinduced microchannels in silicon was different from that in transparent materials, which probably arose from the competition between self-focusing due to the nonlinear Kerr effect and self-defocusing related to the thermal accumulation in the process of laser irradiation.

PACS 42.65.-k · 52.38.-r

1 Introduction

Silicon, as the most important material for the semiconductor industry, has a widespread application in electronic devices and microelectromechanical systems. As one of the most effective micromachining means, femtosecond laser

interaction with silicon has been studied during the last few years [1–3]. Most of the studies focused on high-precision drilling and cutting for the fabrication of complex surface patterns. There are few investigations to demonstrate the interior fabrication of silicon using a femtosecond laser. This is due to the fact that silicon is a strong absorber of the near-infrared and visible-light regions, which makes it difficult to induce and observe microstructures in the interior of silicon.

Nejadmalayeri et al. reported a buried waveguide induced in silicon by a femtosecond laser at 2.4 μm, which extends the ultra-fast three-dimensional modification technique to silicon [4]. Recently, we demonstrated photoinduced microstructures in the interior of silicon wafers using an 800-nm femtosecond laser, which showed the possibility of three-dimensional fabrication inside silicon using 800-nm femtosecond laser pulses [5].

In this letter, we report on photoinduced multiple microchannels in the interior of silicon produced using a femtosecond laser of 800-nm wavelength, which is in the absorption region of silicon. The multiple microchannels were aligned spontaneously with a period along the propagation direction of the laser beam, which phenomenon could be attributed to the interface spherical aberration induced due to refractive-index mismatch when a tightly focused laser propagated through an interface of two different materials. We also observed that the depth of the photoinduced microchannels increased with the increase of the laser power. The power dependence of the depth of photoinduced microchannels in silicon was different from that in transparent materials, which probably arose from the competition between self-focusing due to the nonlinear Kerr effect and self-defocusing related to the thermal accumulation in the process of laser irradiation.

C. Li · X. Shi · J. Si (✉) · F. Chen · T. Chen · Y. Zhang · X. Hou
Key Laboratory for Physical Electronics and Devices
of the Ministry of Education, Shaanxi Key Lab of Information
Photonic Technique, School of Electronics and Information
Engineering, Xi'an Jiaotong University, Xianning-xilu 28,
Xi'an 710049, China
e-mail: jinhaisi@mail.xjtu.edu.cn

F. Chen
e-mail: chenfeng@mail.xjtu.edu.cn

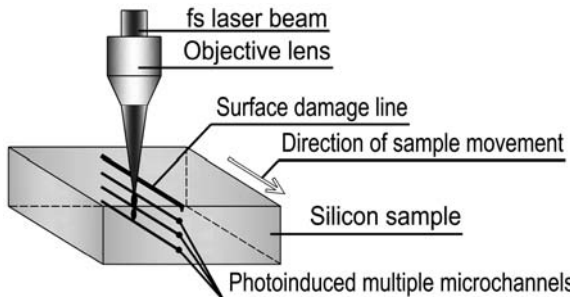


Fig. 1 Schematic setup for the fabrication of the photoinduced multiple microchannels

2 Experiments

The thickness of the silicon wafer used in the experiment is 300 μm . A regeneratively amplified Ti:sapphire laser system was used, which delivered pulses with duration of 30 fs, center wavelength at 800 nm, and repetition rate of 1 kHz. The laser beam was focused inside the silicon wafer by a microscope objective. The energy of the incident pulses could be continuously varied by a variable attenuator. A mechanical shutter was employed to control the access of the laser beam. The silicon wafer was mounted on a computer-controlled three-dimensional translation stage with a resolution of 0.04 μm .

Figure 1 shows the schematic setup for the fabrication of multiple microchannels. A $\times 50$ microscope objective with numerical aperture of 0.50 was employed, which focused the laser pulses below the surface of the silicon wafer. By translating the stage, damage lines were produced on the surface of silicon. The silicon surface perpendicular to the scan direction was polished at a random position and cleaned with alcohol. We observed the photoinduced microchannels on the polished surface through an optical microscope with a $\times 50$ microscope objective using a CCD camera. Moreover, the morphology of the end view of the photoinduced microchannels was characterized with scanning electron microscopy (SEM).

3 Results and discussion

First, we observed periodically aligned multiple microchannels in the interior of silicon. Figure 2a, b, and c show optical microscope photographs of the end view of photoinduced microchannels inside the silicon wafer, in which the laser power was set at 1.0 mW, 1.5 mW, and 2.5 mW, respectively. The laser beam was focused at a geometrical depth of 5 μm from the entrance surface and the scan velocity was set at 15 $\mu\text{m}/\text{s}$. From Fig. 2, we can see that the number of the photoinduced multiple microchannels increased with the increase of laser average power. The photoinduced microchannels have almost a circular cross-sectional shape, and the

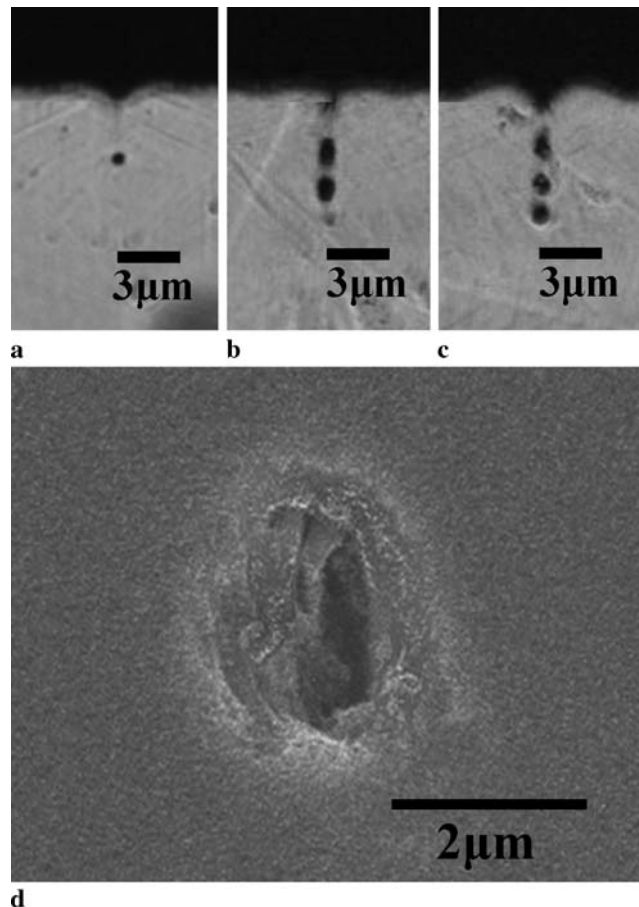


Fig. 2 Optical microscope photographs of end view of the photoinduced microchannels at different laser powers: (a) 1.0 mW, (b) 1.5 mW, and (c) 2.5 mW. The SEM micrograph of the end view of the photoinduced microchannel is shown in (d)

neighboring two voids are independent of each other. The diameter of the microchannels is about 1 μm . The increase of laser power has no obvious influence on the diameter of the microchannels. For transparent glass materials, usually, the continuity of the microchannels can be confirmed by injecting water into the microchannels. For the opaque silicon material, it is difficult to confirm the empty microchannels by injecting water. In our experiments, the microchannels shown above were observed by polishing the sample at a random position, indicating that the microchannels have a good level of continuity. Figure 2d illustrates a SEM micrograph of the end view of the photoinduced microchannels. From Fig. 2d, we can see that the photoinduced microchannel is a through-channel structure. The interior surface of the microchannels is rough and there is some debris in the microchannels. The multiple microchannels can be produced not only by using a $\times 50$ microscope objective but also by using a $\times 10$ or $\times 20$ microscope objective in our experiments. The number of photoinduced microchannels can be controlled not only by changing the laser power but also by changing the scan velocity. Moreover, the depth of the pho-

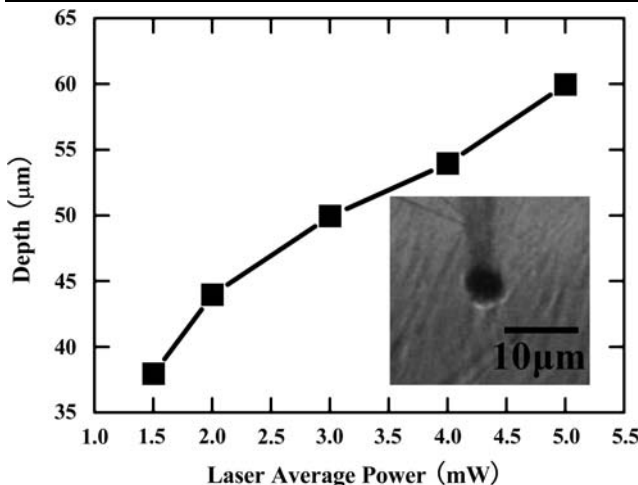


Fig. 3 Dependence of the depth of the photoinduced microchannels on the laser power when the laser beam was focused at 15- μm geometrical depth below the silicon surface and the laser scan velocity was set at 5 $\mu\text{m}/\text{s}$. *The inset* shows the photoinduced microchannel, where the laser average power was set at 2.0 mW

toinduced microchannels can be controlled by varying the laser power. To our knowledge, the femtosecond laser direct writing of multiple microchannels inside silicon has not been investigated in existing references; we expect that the technology of photoinduced multiple microchannels inside silicon can be applied in the fabrication of photonic crystals, silicon microchannel plates, and microchannel heat exchangers.

To investigate the dependence of the depth of the photoinduced microchannels on the laser power, we firstly fabricated a single microchannel inside silicon by setting suitable focal position and scan velocity. The experimental results are shown in Fig. 3, in which the laser power was set at 1.5 mW, 2.0 mW, 3.0 mW, 4.0 mW, and 5.0 mW, respectively. The laser beam was focused at 15- μm geometrical depth below the silicon surface and the laser scan velocity was set at 5 $\mu\text{m}/\text{s}$. The inset of Fig. 3 shows the photoinduced microchannel at the laser power of 2.0 mW. From the inset, we can see that a black line appeared between the entrance surface and the microchannel. The black line inside the wafer was attributed to photoinduced refractive-index change [6, 7]. From Fig. 3, we can see that the depth of the microchannels increased with the increase of the laser power. The power dependence of the depth of the photoinduced microchannels in silicon was different from that in transparent materials [8]. When a femtosecond laser beam was focused in the silica sample, which was transparent to the 800-nm laser, due to the self-focusing related to the Kerr effect, the depth of the focal point of the laser beam inside the silica sample was less than the geometrical focal point, and decreased with the increase of the laser power. When the 800-nm femtosecond laser beam was introduced

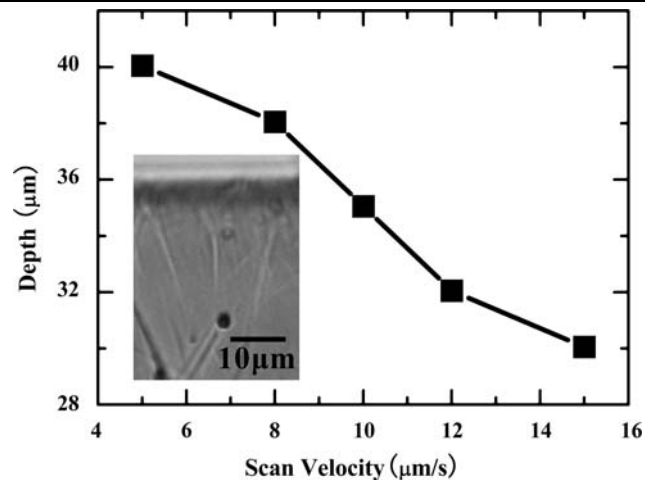


Fig. 4 Dependence of the depth of the photoinduced microchannels on the laser scan velocity when the laser beam was focused at 15- μm geometrical depth below the silicon surface and the laser average power was set at 3 mW. *The inset* shows the photoinduced microchannel, where the laser scan velocity was kept at 15 $\mu\text{m}/\text{s}$

into the silicon material, which was absorptive to the 800-nm laser, not only self-focusing, but self-defocusing due to the thermal accumulation had also a significant influence on the focal-point position of the laser beam [9]. Therefore, the power dependence of the depth of the photoinduced microchannels could be attributed to the competition between self-focusing and self-defocusing. With the increase of the laser power, the thermal accumulation increased and the influence of the self-defocusing effect on the propagation of the laser beam became more and more significant, which made the laser beam focus at a deeper position in the silicon wafer.

To further understand the power dependence of the depth of the photoinduced microchannels observed in silicon, we also studied the dependence of the depth of the photoinduced microchannels on the scan velocity by changing the scan velocity. The results are shown in Fig. 4, in which the laser beam was focused at 15- μm geometrical depth below the silicon surface and the laser average power was set at 2.5 mW. When the scan velocity was increased from 5 $\mu\text{m}/\text{s}$ to 15 $\mu\text{m}/\text{s}$, the depth of the photoinduced microchannels decreased from 40 μm to 30 μm . From Fig. 4, we can see that the depth of the photoinduced microchannels decreased with the increase of the laser scan velocity. The increase of scan velocity means that the number of laser pulses irradiated at the same position of the wafer decreased. For the slower scan velocity, more laser pulses penetrated silicon, and self-defocusing due to thermal accumulation became more significant, which weakened the self-focusing of the laser beam and made the position of the focal point deepen. Therefore, the experimental results demonstrated that the thermal accumulation has an influence on the depth of the photoinduced microchannels, which is consistent with the

results about the power dependence of the depth of the photoinduced microchannels.

According to the results described above, we can conclude that the depth of the photoinduced microchannels can be controlled by changing laser power or laser scan velocity. When the laser power exceeds a critical power, the multiple microchannels can be produced.

The formation of the microchannels could be explained with the micro-explosion model [10, 11]. The laser pulses created high-density electronic plasma in the focal volume, which transferred its excess energy to the lattice. The focal volume was heated to a high temperature. The rise in temperature at a constant volume caused immense pressures and the pressures forced material from the center of the explosion outside. During cooling, the material did not anneal and a denser phase was frozen in. Therefore, a cavity, surrounded by a region of denser material, was formed in the micro-explosion, and some debris was deposited in the microchannels. In addition, some models such as the standing electron plasma wave mechanism [12], multiple refocusing [13], and the spherical aberration effect [14] were proposed to explain the generation of periodic voids induced in transparent materials. However, the spherical aberration effect is commonly considered to be the main mechanism of the formation of the periodic voids in glass [15, 16]. The laser beam was focused by the microscope objective across the air–silicon interface into the silicon. Due to the refractive-index difference between air and silicon, such index mismatch at the air–silicon interface may deflect the laser light and make the focusing depth shift. For transparent materials such as glass, photoinduced multiple microchannels produced due to the spherical aberration effect could usually be induced at depths of more than 100 μm away from the entrance surface using a higher numerical aperture microscope objective [14]. In addition, when the pulse energy was high enough, the Kerr self-focusing effect also has an influence on the position of multiple microchannel onset in the interaction process, which makes the position of the multiple microchannel onset move towards the entrance surface of the sample [17]. Our experiments show that multiple microchannels in silicon could be induced at the depths of less than 50 μm away from the entrance surface using a $\times 50$ microscope objective. Compared with glass, the smaller depth of the photoinduced multiple microchannels in silicon can probably be attributed to the higher refractive index of silicon and the strong absorption at 800 nm. The absorption of silicon at 800 nm restricts the formation of photoinduced multiple microchannels at deeper positions. Therefore, we suggest that for the formation of multiple photoinduced microchannels in silicon, the interface spherical aberration effect induced by the air–silicon interface plays an important role in the nonlinear interaction between the tightly focused laser pulse and the sample. To our knowledge,

up to now, photoinduced multiple microchannels were observed almost always in transparent materials, such as glass [18–21]. We have observed photoinduced multiple microchannels in the interior of silicon using a femtosecond laser of 800-nm wavelength, which is in the absorption region of silicon.

4 Conclusions

In conclusion, periodically aligned multiple microchannels have been fabricated inside silicon by using a femtosecond laser. The multiple microchannels were aligned spontaneously with a period along the propagation direction of the laser beam. The dependences of the depth of the photoinduced microchannels on laser power and scan velocity were also studied.

Acknowledgements The authors gratefully acknowledge the financial support for this work provided by the National Science Foundation of China under the Grant No. 10674107, the National High Technology R&D Program of China under the Grant No. 2009AA04Z305, the National Key Scientific Research Foundation of China under the Grant No. 2006CB921602, and the Specialized Research Fund for the Doctoral Program of Higher Education of China under the Grant No. 200806980022.

References

1. M.Y. Shen, C.H. Crouch, J.E. Carey, E. Mazur, *Appl. Phys. Lett.* **85**, 5694 (2004)
2. T. Tomita, Y. Fukumori, K. Kinoshita, S. Matsuo, S. Hashimoto, *Appl. Phys. Lett.* **92**, 013104 (2008)
3. S. Matsuo, T. Fujine, K. Fukuda, S. Juodkazis, H. Misawa, *Appl. Phys. Lett.* **82**, 4283 (2003)
4. A.H. Nejadmalayeri, P.R. Herman, J. Burghoff, M. Will, S. Nolte, A. Tünnermann, *Opt. Lett.* **30**, 964 (2005)
5. T. Chen, J. Si, X. Hou, S. Kanehira, K. Miura, K. Hirao, *Appl. Phys. Lett.* **93**, 051112 (2008)
6. W. Liu, S.L. Chin, O. Kosareva, I.S. Golubtsov, V.P. Kandidov, *Opt. Commun.* **225**, 193 (2003)
7. S.L. Chin, A. Brodeur, S. Petit, O.G. Kosareva, V.P. Kandidov, *J. Nonlinear Opt. Phys. Mater.* **8**, 121 (1999)
8. A. Saliminia, N.T. Nguyen, S.L. Chin, R. Vallée, *Opt. Commun.* **241**, 529 (2004)
9. Y.R. Shen, *The Principles of Nonlinear Optics* (Wiley, New York, 1984)
10. S. Juodkazis, H. Misawa, T. Hashimoto, E.G. Gamaly, B. Luther-Davies, *Appl. Phys. Lett.* **88**, 201909 (2006)
11. W.G. Roeterdink, L.B.F. Juurink, O.P.H. Vaughan, J.D. Diez, M. Bonn, A.W. Kleyn, *Appl. Phys. A* **82**, 4190 (2003)
12. H. Sun, J. Song, C. Li, J. Xu, X. Wang, Y. Cheng, Z. Xu, J. Qiu, T. Jia, *Appl. Phys. A* **88**, 285 (2007)
13. Z. Wu, H. Jiang, L. Luo, H. Guo, H. Yang, Q. Gong, *Opt. Lett.* **27**, 448 (2002)
14. A. Marcinkevicius, V. Mizeikis, S. Juodkazis, S. Matsuo, H. Misawa, *Appl. Phys. A* **76**, 257 (2003)
15. C. Mauclair, A. Mermilliod-Blondin, N. Huot, E. Audouard, R. Stoian, *Opt. Express* **16**, 5481 (2008)
16. J. Song, X. Wang, X. Hu, Y. Dai, J. Qiu, Y. Cheng, Z. Xu, *Appl. Phys. Lett.* **92**, 092904 (2008)

17. Q. Sun, H. Jiang, Y. Liu, Y. Zhou, H. Yang, Q. Gong, J. Opt. A: Pure Appl. Opt. **7**, 655 (2005)
18. R. An, Y. Li, Y. Dou, H. Yang, Q. Gong, Opt. Express **13**, 1855 (2005)
19. J.P. McDonald, V.R. Mistry, K.E. Ray, S.M. Yalisove, Appl. Phys. Lett. **88**, 183113 (2006)
20. E. Toratani, M. Kamata, M. Obara, Appl. Phys. Lett. **87**, 171103 (2005)
21. S. Kanehira, J. Si, J. Qiu, K. Fujita, K. Hirao, Nano Lett. **5**, 1591 (2005)